The Journal of Neuroscience, May 1, 2002, 22(9):3426–3433

Ca^{2+}-Independent Feedback Inhibition of Acetylcholine Release in Frog Neuromuscular Junction

Inna Slutsky, Grigory Rashkovan, Hanna Parnas, and Itzchak Parnas

The Otto Loewi Minerva Center for Cellular and Molecular Neurobiology, Department of Neurobiology, The Hebrew University, Jerusalem 91904, Israel

The effect of membrane potential on feedback inhibition of acetylcholine (ACh) release was studied using the frog neuromuscular junction. It was found that membrane potential affects the functional affinity (K_i) of the presynaptic M_2 muscarinic receptor. The K_i for muscarine shifts from ~0.23 μM (at resting potential) to ~8 μM (at a high depolarization). Measurements of Ca^{2+} currents in axon terminals showed that the depolarization-mediated shift in K_i does not stem from depolarization-dependent changes in Ca^{2+} influx. Pretreatments with pertussis toxin (PTX) abolished the depolarization-dependent shift in K_i; at all depolarizations K_i was the same and higher (~32 μM) than before PTX treatment. The inhibitory effect of muscarine on ACh release is produced by two independent mechanisms: a slow, PTX-sensitive process, which prevails at low to medium depolarizations and operates already at low muscarine concentrations, and a fast, PTX-insensitive and voltage-independent process, which requires higher muscarine concentrations. Neither of the two processes involves a reduction in Ca^{2+} influx.

Key words: feedback inhibition; M_2 muscarinic presynaptic receptor; frog neuromuscular junction; Ca^{2+} currents; Ca^{2+}-independent inhibition; fast and slow inhibition

Feedback inhibition of ACh release is achieved via presynaptic G-protein-coupled muscarinic receptors (for review, see Starke et al., 1989; Caulfield, 1993). Of the five known muscarinic receptor subtypes (M_1–M_5), the M_2 receptor (M_2R), which is most abundant at presynaptic nerve terminals in the CNS (Rouse and Levey, 1997; Rouse et al., 2000), is involved in feedback inhibition (Allen and Brown, 1993; Bellingham and Berger, 1996; Slutsky et al., 1999).

M_2Rs may affect ACh release by a reduction in Ca^{2+} current, achieved by more than one mechanism (for review, see Hille, 1994; Zamponi and Snutch, 1998) (Patil et al., 1996; Roche and Treistman, 1998). One process, the membrane-delimited inhibition of Ca^{2+} channels, is fast, it is voltage-dependent and pertussis toxin (PTX)-sensitive, and operates by interaction of G-$\beta\gamma$ subunits (Herlitze et al., 1996; Ikeda, 1996), with N- and P/Q-type Ca^{2+} channels (Zhang et al., 1996; Zamponi et al., 1997). The second, a slow process, is voltage-independent and PTX-insensitive and operates via an unknown second messenger (Bernheim et al., 1991; Beech et al., 1992).

In many of the studies cited above, Ca^{2+} currents were measured in cell bodies, rather than nerve terminals or in various cell lines in which Ca^{2+} channels and M_2Rs were both expressed and long depolarizing pulses and relatively high concentrations of ACh were used (but see Hamilton and Smith, 1991). For example, it was recently reported that 50 μM ACh (equivalent to 250 μM muscarine, Birdsall et al., 1978) reduced Ca^{2+} currents elicited by $\geq$100 msec depolarizing pulses in *Xenopus* oocytes in a voltage-dependent manner; inhibition of Ca^{2+} current being stronger the lower the depolarization (Patil et al., 1996; Roche and Treistman, 1998). Also, in some of these studies measurements of Ca^{2+} currents were not accompanied with measurements of transmitter release. Hence, these studies do not exclude the possibility that concentrations of muscarine (or ACh), which do not affect Ca^{2+} currents, inhibit, nevertheless, ACh release.

In other studies, focusing on effects of muscarine on release of ACh, it was suggested that the feedback inhibition of ACh release operates, presumably in addition to the above, by mechanisms that do not affect Ca^{2+} entry (Muller et al., 1987; Dolezal and Tućek, 1993; Scanziani et al., 1995; Slutsky et al., 1999). Furthermore, such "Ca^{2+}-independent" inhibition, like the membrane-delimited inhibition of Ca^{2+} channels, was found to be voltage-dependent. Inhibition was strong at low depolarization and it diminished as depolarization increased (Dolezal and Tućek, 1993; Slutsky et al., 1999).

In the present work we attempt to unravel the mechanisms that underlie feedback inhibition of ACh release that is not mediated by reduction in Ca^{2+} entry. Using the frog neuromuscular junction (NMJ), we found that the inhibition of ACh release, which does not involve a reduction in Ca^{2+} entry, includes two distinct processes. One, voltage-dependent and PTX-sensitive, is characterized by a slow time course and a high affinity toward muscarine. The other, voltage-independent and PTX-insensitive, exhibits significantly faster kinetics and is of low affinity toward muscarine.

MATERIALS AND METHODS

Preparation and solutions. Frogs (*Rana ridibunda*) were killed by stunning followed by double pitting according to the institution guidelines and the Israeli law for protection of animals. The cutaneous pectoris nerve muscle preparation was isolated and secured with small insect pins in a chamber with sylgard bottom and shallow walls ($4 \times 2 \times 0.4$ cm^3). The chamber was attached to a stage of an upright microscope (Zeiss, Oberkochen, Germany; axioscope), which was modified to also hold the micromanipulators and other attachments. The nerve terminals were viewed by a 40× long distance objective with working distance of 1.8 mm.

Received Nov. 28, 2001; revised Feb. 20, 2002; accepted Feb. 20, 2002.

This work was supported by Deutsche Forschungsgemeinschaft (Germany) Grant SFB 391 (J.D., I.P.). We are grateful to the Goldie Anna fund for their continuous support. I. P. is the Greenfield Professor of Neurobiology.

Correspondence should be addressed to Itzchak Parnas, Department of Neurobiology, The Hebrew University, Jerusalem 91904, Israel. E-mail: ruthy@vms.huji.ac.il.

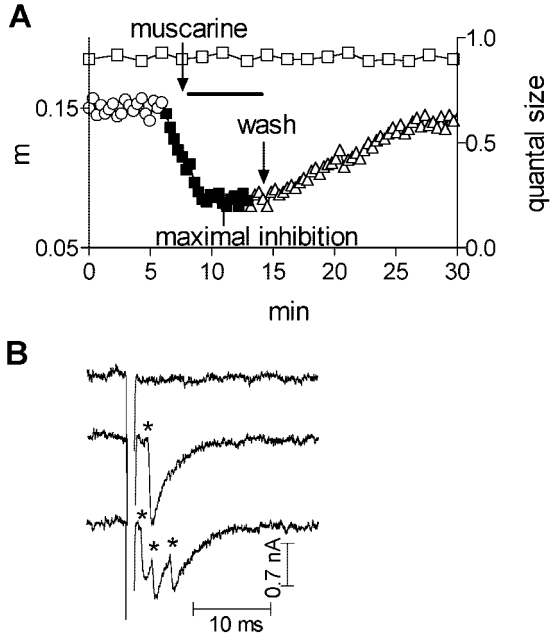

Figure 1. *A*, Time dependence of quantum size (□, *right y*-axis) and of quantal content (*m*, *left y*-axis) in control (○), after addition of 1 μM muscarine (■), and after wash (△). The *topmost arrow* points to the time at which muscarine reached the chamber. The *bottommost arrow* points to the beginning of wash. *B*, Samples of traces. Quanta events are marked by *asterisks*.

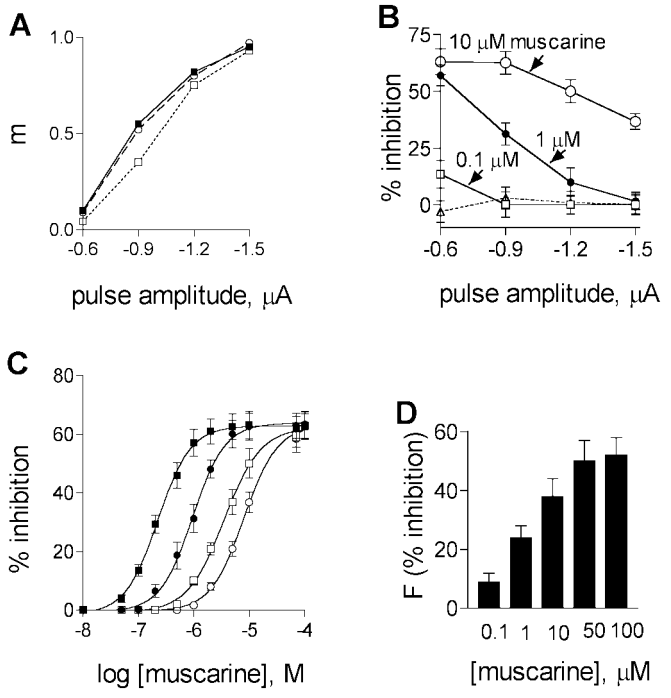

Figure 2. Effects of muscarine on evoked and asynchronous ACh release. *A*, Quantal content in control (■), after addition of 1 μM muscarine (□), and after washing (○). *B*, Average percentage of inhibition of ACh release by different concentrations of muscarine at four pulse amplitudes ($n = 6$): 0.1 μM, □; 1 μM, ●; 10 μM, ○. *Stippled line* shows recovery after wash. *C*, Dose–inhibition curves at different pulse amplitudes: −0.6 μA, ■; −0.9 μA, ●; −1.2 μA, □; −1.5 μA, ○. The average K_i values ($n = 6$) for the four pulse amplitudes are given in Table 1. *Curves* were fitted by the sigmoidal dose–response (variable slope) equation by Graph PadPrism software ($R^2 > 0.9$). *D*, Effect of different concentrations of muscarine on the frequency of asynchronous ACh release, *F* (sec^{-1}) ($n = 8, p < 0.001$).

This allowed us to place a macropatch electrode (see below) over a terminal under visual control. The chamber was constantly perfused (Gilson, Middleton, WI; minipulse 3 pump) with the bathing solution, which passed through a heat exchanger. Temperature was kept at 8 ± 1°C. The bathing solution contained (in mM): NaCl 116, KCl 2, $MgCl_2$1, $CaCl_2$ 1, and HEPES 2. The pH was adjusted to 7.4 by adding NaOH. All experiments were done in the presence of 10–50 μM pirenzepine, a selective antagonist of the M_1 receptors ($K_{d,}$ ~10 nM; McKinney et al., 1989; Caulfield, 1993) to block enhancement of ACh release at frog NMJ (Slutsky et al., 1999).

Stimulation and recording. For focal depolarization, we used a macropatch electrode (Dudel, 1981; Dudel et al., 1993) pulled from 2 mm hematocrit capillaries. The short working distance enforced an almost horizontal approach, and thus the use of an electrode with a long shaft and a bent tip (Ravin et al., 1997). The tip (~6–8 μm opening) was placed over a branch of the endplate. Pulse duration was usually 0.7 msec, and pulse amplitude varied between −0.6 and −1.5 μA. Although the exact level of depolarization is not known, it increases with the pulse amplitude (Dudel, 1981). Stimulation frequency was 3 Hz. To enable graded depolarization of the terminal (Dudel, 1981), 0.2 μM TTX was added to prevent sodium excitability.

For action-potential evoked release, the axon was stimulated by a suction electrode, and postsynaptic currents (EPSCs) were recorded with a macropatch electrode. Pulse duration was 0.2 msec, and pulse amplitude was ~50% above threshold. Stimulation frequency was 1 Hz. In these experiments 2 μM D-tubocurarine (D-TC) was added to prevent muscle contraction.

For intracellular recording of postsynaptic potentials we used conventional techniques. Microelectrodes were pulled from 2 mm glass capillaries (Clark Electromedical Instruments, Reading, UK) and filled with 3 M KCl. Electrode resistance was 8–10 MΩ. The Axoclamp (Axon Instruments, Foster City, CA) was used as an amplifier.

Determination of quantal content. Quanta were recorded with a macropatch electrode (Dudel, 1981). At 8°C, the quanta appear after the stimulus artifact, and the desynchronized release enables easy detection of the single quanta (Fig. 1*B*). To determine the quantal content, the quanta were counted for a period of 10 msec after the beginning of the depolarization artifact. The number of counted quanta divided by the number of applied pulses yields directly the quantal content (for more details, see Slutsky et al., 1999). Asynchronous release was measured starting 10 msec after the depolarizing pulse until the following pulse (320 msec). To analyze the data, analog-to-digital conversion at 50 kHz was done using the Labview (AT-MIL-16F-5, NI-DAQ 4.9.0 driver software) interface.

The basic experiment. The terminal was stimulated at 3 Hz, at which the number of applied pulses varied according to the desired range of quantal content (but at least 256 pulses were applied), and the control quantal content (Fig. 1*A*, *open circles*) was established. Then, muscarine was added (Fig. 1*A*, *filled squares*) to the perfusion solution, and the quantal content was again monitored. When the quantal content stabilized at the lowest level (maximal inhibition), the preparation was washed (Fig. 1*A*, *open triangles*), and recovery from inhibition was seen. Such experiments require stable recording from the same site. To ensure existence of stability, two criteria were checked. First, if the seal resistance changed by >10%, the experiment was discarded. Second, because the amplitude and the shape of single quanta events are sensitive to even small movements of the electrode, the average amplitude of the single quanta (examples seen in Fig. 1*B*) was continuously monitored. It can be seen (Fig. 1*A*, *open squares*) that the quantum size did not change during the entire experiment.

The alternate stimulation protocol: establishing dose–inhibition curves. To establish the muscarine concentration at which 50% inhibition is obtained (functional affinity or K_i), full dose–inhibition curves (DI) must be measured for each pulse amplitude (Fig. 2*C*). Each data point on the various DI curves corresponds to the maximal inhibition achieved in the basic experiment at the relevant muscarine concentration. It follows that if the DI curves at the various pulse amplitudes would be measured in a sequential order, a long time would elapse between the time of measuring the first, and say, the last DI curve, which may distort the true dependence of the K_i on the pulse amplitude. To ensure that this is not the case and that the quantal contents at the various pulse amplitudes are measured approximately at the same time, the alternate stimulation protocol had been used.

Four depolarizing pulses of different amplitudes (−0.6, −0.9, −1.2, −1.5 μA) were administered in a random manner, and the control quantal contents were determined. The interval between pulses was 300 msec. Stimulation was continuous to allow accumulation of responses of 500–2000 pulses. Then, the lowest concentration of muscarine was added, and after 10 min, a period that is sufficient to produce maximal inhibition (Fig. 1*A*) (Slutsky et al., 1999), the same depolarizing pulses as for the control were again administered. The same procedure was repeated for seven additional muscarine concentrations, applied in an increasing order. The preparation was then washed to achieve recovery. Only those experiments that showed at least 90% recovery were taken for analysis. It should be emphasized that all these measurements were done on one and the same release region. Thus, for each successful experiment we obtained the effects of eight concentrations of muscarine at four pulse amplitudes.

Ca^{2+} current measurement. Presynaptic Ca^{2+} currents were measured with a macropatch electrode from a small region just below the electrode rim as close as possible to a release site (Brigant and Mallart, 1982; Slutsky et al., 2001). To isolate Ca^{2+} currents, the following procedure was used. Because of the long shaft of the macropatch electrode we could not achieve block of the inward sodium current by perfusion of the tip of the electrode with agents that block sodium currents, as done by Slutsky et al. (1999). Instead, 20 μM TTX was added to the electrode. With such a high concentration, a sufficient amount of TTX diffused out to block sodium excitability at the membrane below the electrode and possibly in its vicinity. This was ascertained by giving brief (0.2 msec) graded depolarizing pulses. When the electrode contained TTX, a graded release was seen. In contrast, when the electrode did not contain TTX, an "all or none" jump in release was obtained, providing that threshold was achieved. Having TTX only in the electrode enabled propagation of an action potential to the region of the recording, on one hand, and block of the Na^+ currents at the recording site and its close proximity, on the other hand, and thereby enabling a better detection of the Ca^{2+} currents. Tetraethylamonium chloride (TEA; 10 mM) and 3,4-diaminopyridine (3,4-DAP; 100 μM) were then added to the circulating fluid to block K^+ currents, leaving Ca^{2+} and capacitative currents. This probably broadened the action potential, but subtraction of the traces before and after addition of cadmium (100 μM) yielded the Ca^{2+} current in isolation.

Drugs and chemicals. TTX was purchased from Alamone Labs (Jerusalem, Israel); PTX, B-Oligomer, and pirenzepine were from RBI (Natick, MA); D-TC, TEA, and 3,4 DAP were from Sigma (St. Louis, MO).

Statistical evaluation. Significance was checked by paired or unpaired two-tailed *t* test. Results are given as mean ± SEM. The K_i parameters were evaluated using a standard least-squares-sum fit technique provided by the GraphPad Prism software. Goodness of fit was quantified by the value R^2 (fit is good when $R^2 > 0.9$). Best-fit K_i values were compared by unpaired one-tailed *t* test.

RESULTS

Dependence of K_i on pulse amplitude

One experiment showing the effect of 1 μM muscarine on ACh release at four pulse amplitudes is seen in Figure 2*A*. In the control (*filled squares*), the quantal content (*m*) increased from a value of 0.1 at the low depolarizing pulse (−0.6 μA) to a value of 0.95 at the high depolarizing pulse (−1.5 μA). After addition of 1 μM muscarine (*open squares*, each data point represents the maximal inhibition) *m* decreased to 0.04 at the low depolarizing pulse, but remained 0.93 at the high depolarizing pulse. After washing with normal Ringer's solution, the dependence of the quantal content on pulse amplitude was as in the control (*open circles*). Experiments, as the one described in Figure 2*A*, were performed with several muscarine concentrations, and the results of such experiments ($n = 6$) are shown in Figure 2*B*. Here, percentage of inhibition from the control value is presented for three concentrations of muscarine at the four pulse amplitudes. Figure 2*B* shows that for each pulse amplitude, inhibition increases as muscarine concentration increases, but at the lowest pulse amplitude inhibition reached saturation (~60%) already at a muscarine concentration of 1 μM. Figure 2*B* also illustrates that inhibition of ACh release is voltage-dependent. For the muscarine concentrations used in Figure 2*B*, inhibition is strong at low pulse amplitudes, and it weakens as the pulse amplitude increases (Slutsky et al., 1999). At the high pulse amplitude, inhibition is even fully abolished, providing that muscarine concentration is low. Recovery was achieved after ~30 min wash (Fig. 2*A*, *stippled line*).

Table 1. K_i values for muscarine at four pulse amplitudes at different experimental conditions

	K_i values (μM)		
Depolarizing pulse amplitude	Control ($n = 6$)	PTX-treated ($n = 6$)	B-oligomer-treated ($n = 4$)
−0.6 μA	0.23 ± 0.03	31.0 ± 2.6	0.19 ± 0.05
	***	*	***
−0.9 μA	0.95 ± 0.1	31.8 ± 4.3	0.92 ± 0.1
	***	*	***
−1.2 μA	3.5 ± 0.4	32.5 ± 4.2	3.8 ± 0.4
	**	*	**
−1.5 μA	8.0 ± 0.9	33.1 ± 3.1	8.1 ± 0.9

K_i values obtained at two depolarization levels were compared by unpaired one-tailed *t* test. The significance for difference between K_i values for each column for two successive pulse amplitudes is given: *insignificant difference ($p > 0.4$); **significant difference ($p < 0.05$); ***highly significant difference ($p < 0.001$). The difference for the minimal and the maximal pulse amplitudes in both the control and in B-oligomer-treated preparations was highly significant ($p < 0.0001$). The difference between control and PTX-treated preparations was highly significant ($p < 0.0001$) for each pulse amplitude. The difference between controls and B-oligomer-treated preparations was insignificant ($p > 0.5$) for each pulse amplitude.

Figure 2*C* and Table 1 depict results of six experiments of the type seen in Figure 2, *A* and *B*, drawn in the form of DI curves for four pulse amplitudes (see Materials and Methods for experimental protocol). It is seen that as the pulse amplitude increases, the DI curves shift to the right; K_i shifted from a value of 0.23 ± 0.03 μM at −0.6 μA (*filled squares*) to a value of 8.0 ± 0.9 μM at −1.5 μA (*open circles*). (We did not try higher pulses to avoid damage of the terminal.) The saturation level of inhibition (~60%) was the same at all pulse amplitudes, but it was achieved at various muscarine concentrations for the various pulses.

Figure 2*D* shows that muscarine inhibited also asynchronous release in a concentration-dependent manner: 0.1 μM muscarine produced inhibition of 9 ± 3% ($n = 8$; $p < 0.001$), and 50 μM muscarine produced inhibition of 50 ± 7% ($n = 8$; $p < 0.001$).

Muscarine at a concentration of 70 μM does not affect presynaptic Ca^{2+} currents

As activation of M_2R was shown to reduce Ca^{2+} current in a voltage-dependent manner (see citations in introductory remarks), it is possible that at high depolarizations, which produce a smaller reduction of Ca^{2+} current, a larger concentration of muscarine is required to reduce the Ca^{2+} current to a level that produces 50% inhibition of release. If this is the case, then the depolarization-induced shift in K_i (seen in Fig. 2*C*) merely reflects a smaller reduction in Ca^{2+} current, at the higher depolarization, rather than a genuine shift in the K_i of the M_2R.

To test for this possibility, direct measurements of Ca^{2+} currents were conducted. Slutsky et al. (1999) found that 10 μM muscarine (in the presence of pirenzepine) did not reduce the presynaptic Ca^{2+} current recorded near a release site, yet at this concentration of muscarine, ACh release was reduced substantially. Because we used, in the present study, higher concentrations of muscarine (up to 70 μM), we checked whether 70 μM muscarine reduce Ca^{2+} currents. Measurement of Ca^{2+} currents

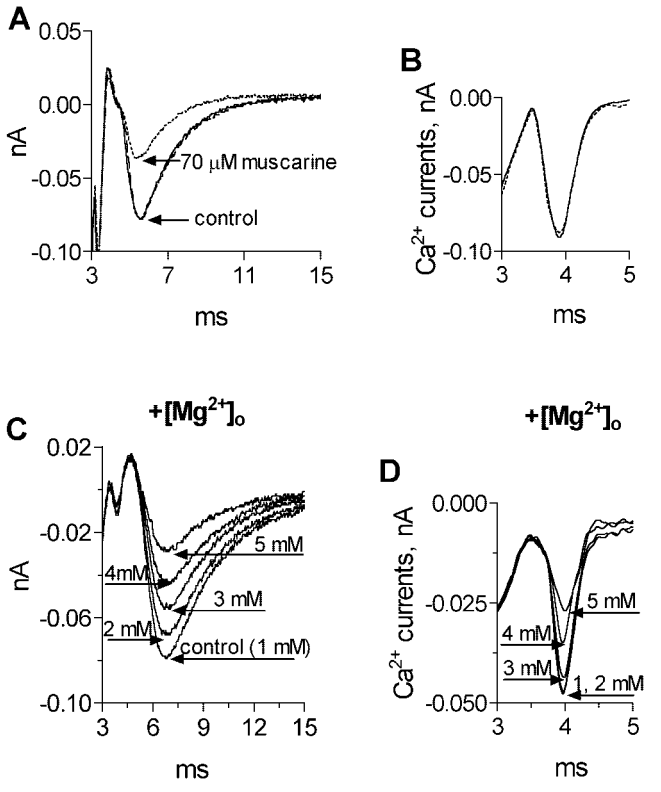

Figure 3. Effects of muscarine and $[Mg^{2+}]_o$ on presynaptic Ca^{2+} currents and EPSCs. *A*, EPSC at control (*solid line*), after addition of 70 μM muscarine (*stippled line*), and after wash (*dashed line*). *B*, Ca^{2+} currents (average of 200 traces) from the same experiment as *A* at control (*solid line*) and after application of 70 μM muscarine (*stippled line*). *C*, EPSCs at different $[Mg^{2+}]_o$. *D*, Ca^{2+} currents (average of 200 traces) from the same experiment as *C*.

requires nerve stimulation (see Materials and Methods) as a result of which an action potential is produced, and hence, the nerve terminal encounters high depolarization. At such high depolarizations, the membrane-delimited inhibition of Ca^{2+} channels is greatly reduced, or may even be completely abolished (Patil et al., 1996; Roche and Treistman, 1998). Hence, the measurements of Ca^{2+} currents using an action potential may not exclude the possibility that under low depolarizations it is the reduction in Ca^{2+} currents that underlies the observed inhibition. To clarify this issue, we measured the effect of 70 μM muscarine on both the EPSC amplitude and the Ca^{2+} currents.

First, we checked the effect of 70 μM muscarine on the EPSC (Fig. 3*A*, in the presence of 2 μM D-TC). As seen, the amplitude of the EPSC was reduced by 53%. Then, after wash and full recovery of the control EPSC, we measured Ca^{2+} currents at the same release region (Fig. 3*B*, in the presence of 10 μM D-TC). It is clearly seen that 70 μM muscarine did not reduce the Ca^{2+} current. On average, 70 μM muscarine reduced the amplitude of the EPSC by 55 ± 8% ($n = 3$; $p < 0.001$), but did not affect the Ca^{2+} currents ($n = 6$; $p > 0.7$).

To check the sensitivity of the method used here for measuring Ca^{2+} currents, we measured Ca^{2+} currents and their corresponding EPSCs at various extracellular Mg^{2+} concentrations, $[Mg^{2+}]_o$.

To do so, we repeated the procedure described for Figure 3, *A* and *B*. The dependence of the EPSCs on $[Mg^{2+}]_o$ is depicted in Figure 3*C,* and the dependence of the Ca^{2+} currents on $[Mg^{2+}]_o$ is seen in Figure 3*D*. A correlation is seen between the reduction in the Ca^{2+} current and the reduction in the amplitude of the EPSC. For example, 3 mM $[Mg^{2+}]_o$ produced a reduction of 7% in the Ca^{2+} current and a reduction of 25% in the corresponding EPSC. As expected, with higher $[Mg^{2+}]_o$ (5 mM), the reduction in the Ca^{2+} current was higher (37%), and the reduction in the corresponding EPSC was larger (54%).

The results in Figure 3 clearly show that the method used here to measure Ca^{2+} currents is sensitive and detects even relatively small changes in Ca^{2+} currents. Therefore, had muscarine affected the Ca^{2+} currents, we would certainly be able to detect it.

Based on the above, we may conclude that under the conditions used here, i.e., action potential-evoked release or brief depolarizing pulses of 0.7 msec duration, the main mechanisms by which muscarine reduces release at concentrations up to 70 μM do not involve a detectable reduction in Ca^{2+} entry.

PTX-catalyzed ADP ribosylation of G-proteins prevents the depolarization-mediated shift in K_i

To check whether G-proteins are involved in the Ca^{2+}-independent depolarization-mediated shift in K_i, muscles were incubated, at 30°C, for a period of 2 hr in a bathing solution (no added Ca^{2+}) containing 1 μg/ml PTX. Then, the muscles were washed with normal bathing solution at 8°C, and the experimental procedure described in Figure 2*A*--*C* was repeated. The results of such experiments are seen in Figure 4.

It is seen that treatment with PTX did not abolish the muscarine-mediated inhibition, but changed radically the dependence of inhibition on membrane potential. In particular, inhibition ceased to be voltage-dependent and was determined solely by muscarine concentration (Fig. 4*A*). Furthermore, on the whole, after PTX treatment, higher concentrations of muscarine were needed to produce the same level of inhibition seen in untreated muscles. For example, after PTX treatment, 1 μM muscarine did not inhibit release (Fig. 4*A,B*), whereas this concentration produced already saturated level of inhibition (60%) at low pulse amplitudes in untreated muscles (Fig. 2*B,C*). Redrawing the data of Figure 4*A* in the form of DI curves (Fig. 4*B*, Table 1) recapitulates the observation that after PTX treatment inhibition became voltage-independent: the K_i was not significantly different for all pulse amplitudes ($n = 6$; $p > 0.4$) (Table 1), and the average K_i was 32 ± 5 μM. This value is higher than the highest K_i (obtained at the high pulse amplitude of −1.5 μA) in untreated muscles (~8 μM).

The results of Figure 2*C* and Figure 4*B* suggest that at any level of depolarization the apparent K_i (Fig. 2*C*) reflects a weighted balance between the high-affinity and the low-affinity processes. At low depolarizations, K_i is low because the high-affinity process prevails. At high depolarizations, the high-affinity process is primarily reduced and hence, the low-affinity inhibition (high K_i) prevails.

The observation that the K_i, after PTX treatment, was even higher than the highest K_i in untreated preparations may indicate that in the latter, even at the highest depolarization used here, the high-affinity process had some contribution to the overall inhibition, and hence, reduced the intrinsic K_i of the low-affinity process.

To show that the effects of PTX are genuine and do not result from the 2 hr of incubation at 30°C, muscles were treated in the same way, but without adding PTX. In such muscles, all parameters remained as in controls (0.20 ± 0.03 at −0.6 μA and 7.9 ± 1.0 at −1.5 μA; $n = 4$; data not shown).

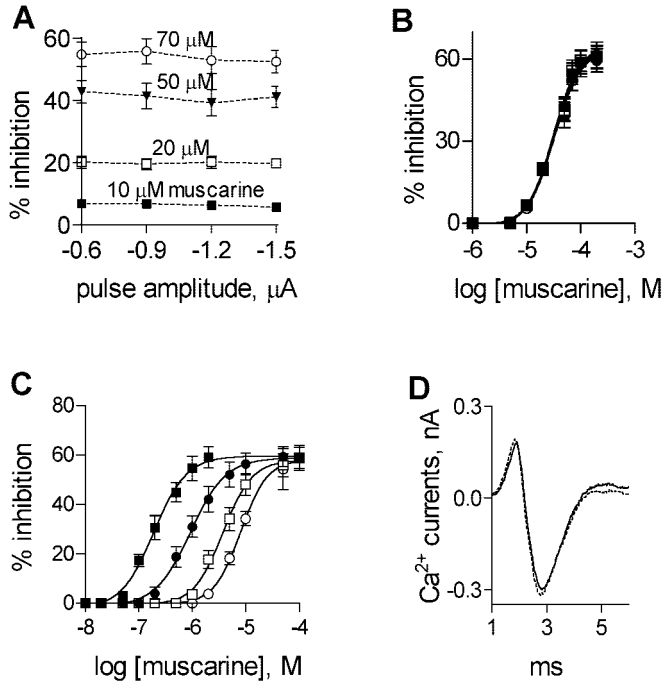

Figure 4. Effects of PTX on muscarine-mediated inhibition of ACh release and on Ca^{2+} currents. *A*, Percentage of inhibition of ACh release at four pulse amplitudes by different muscarine concentrations: 10 μM, ■; 20 μM, □; 50 μM, ▼; 70 μM, ○. *B*, Effect of PTX on DI curves at different pulse amplitudes (the same data as in *A*). Average K_i values ($n = 6$) for the four pulse amplitudes are given in Table 1. *C*, Effect of PTX B subunit on DI curves at different pulse amplitudes: −0.6 μA, ■; −0.9 μA, ●; −1.2 μA, □; −1.5 μA, ○. Average K_i values ($n = 4$) for the four pulse amplitudes are given in Table 1. The curves in *B* and *C* were fitted by the sigmoidal dose–response (variable slope) equation by Graph PadPrism software ($R^2 > 0.9$). *D*, A 100 μM concentration of muscarine had no effect on Ca^{2+} currents at PTX-treated preparation. Control (*solid line);* after addition of 100 μM muscarine (*stippled line*) (average of 200 traces).

To further test whether the effect of PTX resulted from catalytic activity of the PTX A subunit or from another cellular response produced by the PTX B subunit, the B-oligomer was checked for its effect on the depolarization-induced shift of K_i. In these experiments, all preparations were incubated at 30°C for 2 hr in a bathing solution containing 2 μg/ml B-oligomer (without addition of Ca^{2+} ions). Figure 4*C* and Table 1 show that the B-oligomer had no effect on the muscarine-mediated inhibition of ACh release for the entire range of pulse amplitudes. The depolarization-induced shift in the K_i was the same as in untreated preparations ($n = 4$; $p > 0.6$). These results indicate that activation of G_α, which is involved in a second messenger formation, results in the depolarization-induced shift in K_i.

The PTX-independent feedback inhibition is also Ca^{2+}-independent

Ca^{2+} currents were measured as before but now from PTX-treated preparations. Figure 4*D* illustrates superimposed averages (200 sweeps) of Ca^{2+} currents in control (*solid line*) and after addition of 100 μM muscarine (to account for the higher K_i for muscarine under these conditions, *stippled line*). It is seen, similarly to untreated preparations, that muscarine had no effect on the peak Ca^{2+} current in the PTX-treated muscles (Fig. 4*D* and three additional experiments; $p > 0.7$).

Two distinct processes underlie the Ca^{2+}-independent feedback inhibition of ACh release

The finding that low concentrations of muscarine became ineffective after PTX treatment, whereas medium and high concentrations blocked release, but in a voltage-independent manner, raised the possibility that two distinct mechanisms may be involved in producing the Ca^{2+}-independent feedback inhibition of ACh release.

In an attempt to further distinguish between these two putative mechanisms, we measured the time course of evolvement of inhibition under conditions that are likely to selectively expose one or the other process.

Because of the long shaft of the macropatch electrode (attributable to the small working distance), it was impossible to rapidly perfuse the electrode with the drug, as done by Slutsky et al. (1999), and hence, muscarine was added to the reservoir of the circulating fluid. It, therefore, took some time for the muscarine to pass through the inlet tube to reach the chamber containing the muscle. To measure this time, the inlet tube was briefly removed, at the instant that muscarine was added, from the reservoir to suck a bubble of air. It took 90 sec for the air bubble to reach the chamber, and this time corresponds to the time of arrival of the solution containing the muscarine to the chamber. This time was subtracted from the time that elapsed from the addition of muscarine until inhibition was detected. To establish the quantal content, we used, as before, the macropatch recording system. This procedure is rather slow because we normally applied at least 256 pulses to establish one data point, which means that it takes ~1.5 min to evaluate one data point.

In spite of this procedure being a slow one, it could potentially be suitable for measuring the time course of feedback inhibition, because feedback inhibition is known to be a slow process with a time-constant in the range of minutes (Slutsky et al., 1999) (Fig. 1*A*). We, nevertheless, increased somewhat the time resolution by applying only 100 pulses at 3 Hz, such that only 33 sec were now needed to establish one data point.

Selection of the experimental conditions that are likely to discern between the two putative mechanisms is based on the following observations. PTX-untreated preparations showed voltage-dependent inhibition, and inhibition was significant already at low muscarine concentrations. In PTX-treated preparations, both the voltage dependence and the inhibition by low muscarine concentrations disappeared. Therefore, we examined the kinetics of evolvement of inhibition at low (1 μM) and high (50 μM) muscarine concentrations, at low (−0.6 μA) (Fig. 5*A*,*C*) and high (−1.5 μA) (Fig. 5*B*,*D*) pulse amplitudes, without (Fig. 5*A*,*B*), and after treatment with PTX (Fig. 5*C*,*D*). Seen in Figure 5*A* is that the control quantal content fluctuated between 0.11 and 0.13. A 1 μM concentration of muscarine produced maximal inhibition (63%) within 3 min (*filled symbols*), and the quantal content recovered to the control value after wash. Addition of 50 μM muscarine produced maximal inhibition (60%) within 2.6 min (*open symbols*), and here too the quantal content recovered after wash.

When a similar experiment was conducted using a strong depolarizing pulse (−1.5 μA) (Fig. 5*B*), 1 μM muscarine did not reduce release at all; and the quantal content during the control and in the presence of muscarine fluctuated between 1.3 and 1.5 (~10 times higher than the quantal content at the low depolarizing pulse). Addition of 50 μM muscarine produced maximal inhibition (64%) within 1.3 min (*open symbols*).

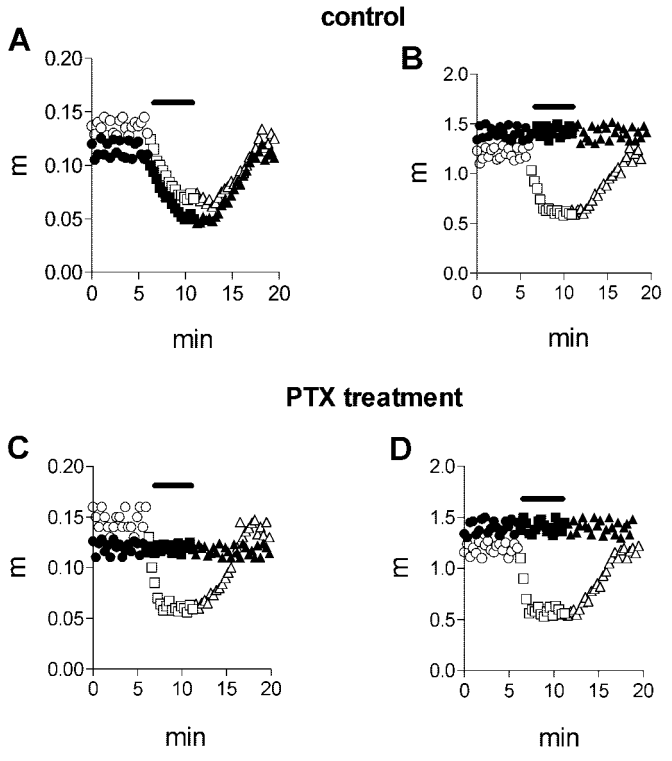

Figure 5. Dependence of the time course of the inhibitory effect of muscarine on pulse amplitude. *Filled symbols*, Experiment with 1 μM muscarine; *open symbols*, experiment with 50 μM muscarine. *Circles,* control; *squares,* after application of muscarine; *triangles,* after wash. The *black bar* indicates the time of application of muscarine. *A*, Effect of muscarine at PTX-untreated preparation at low (−0.6 μA) pulse amplitude. A 1 μM concentration of muscarine produced maximal inhibition within 3 min; 50 μM muscarine produced maximal inhibition within 2.6 min. *B*, Effect of muscarine at PTX-untreated preparation at high (−1.5 μA) pulse amplitude. A 1 μM concentration of muscarine was ineffective; 50 μM muscarine produced maximal inhibition within 1.3 min. *C*, Effect of muscarine at PTX-treated preparation at low (−0.6 μA) pulse amplitude. A 1 μM concentration of muscarine was ineffective; 50 μM muscarine produced maximal inhibition within 1 min. *D*, Effect of muscarine at PTX-treated preparation at high (−1.5 μA) pulse amplitude. A 1 μM concentration of muscarine was ineffective; 50 μM muscarine produced maximal inhibition within 1 min.

When the preparation was incubated with 1 μg/ml of PTX for 2 hr, then, as seen before (Fig. 4), but unlike the situation with PTX-untreated preparation (Fig. 5*A*), 1 μM muscarine did not block release even at the low depolarizing pulse (Fig. 5*C*). A 50 μM concentration of muscarine remained effective and blocked release to about the same level as in Figure 5*A*, but with a faster kinetics: maximal inhibition (62%) was obtained within 1 min. At high depolarization (Fig. 5*D*), the behavior of the PTX-treated preparation resembled that of the untreated one. In both, 1 μM muscarine had no effect, whereas 50 μM muscarine produced a similar block (65% inhibition) within a similar time course. Thus, PTX abolished the slower effect, seen in low depolarization and low concentrations of muscarine (high affinity), although it had no effect on the inhibition seen at high concentrations of muscarine (low affinity, fast effect).

It may be asked why was the fast process not detected at low depolarizations and high muscarine concentration in untreated muscles (Fig. 5*A*, *open symbols*)? As discussed above, Figures 2*C* and 4*B* indicate that at low depolarization, irrespective of muscarine concentration, the high-affinity slow process prevails.

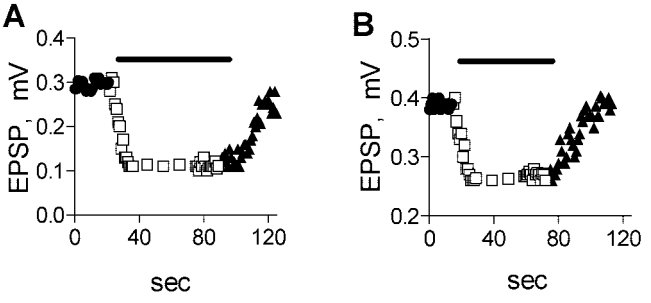

Figure 6. Time course of muscarine-mediated inhibition of action potential-evoked EPSPs. *A*, A 50 μM concentration of muscarine produced maximal inhibition within 13 sec in PTX-untreated preparation. *B*, A 50 μM concentration of muscarine produced maximal inhibition within 12 sec at PTX-treated preparation.

Therefore, the fast process comprises only a small fraction of the total inhibition, and hence could not be detected with the methods used here.

On average, muscarine produced inhibition of ACh release within 2.8 ± 0.5 (n = 7) min at the low pulse amplitude and within 1.4 ± 0.3 (n = 7) min at the high pulse amplitude in PTX-untreated preparations. In PTX-treated preparations, the maximal inhibition was achieved within 1.1 ± 0.3 min (n = 10) at all pulse amplitudes.

Effect of muscarine on action-potential evoked ACh release

The procedure used in Figure 5 to determine the time course of feedback inhibition was suitable for monitoring the time course of the slow process. However, because a minimum of 33 sec is needed to establish one data point of the quantal content, this procedure may not have the needed time resolution to expose the fast process that may well be in the seconds range. To increase the time resolution of our experimental procedure, we resorted to nerve stimulation and intracellular recording of postsynaptic potentials (EPSPs). The EPSP detects release from many sites and its amplitude, because muscarine does not exert postsynaptic effects in this preparation (Slutsky et al., 1999) reflects the quantal content. Hence, at a stimulation rate of 1 Hz, the time resolution of this procedure is 1 sec. Furthermore, in such experiments the NMJ is not covered by a macropatch electrode, and thus it is more exposed to the applied muscarine. We did not use this procedure of intracellular recording in the previous experiments, because it does not enable graded membrane depolarization.

Figure 6*A* shows the amplitude of the EPSP, as it varied in time. During the control, the EPSP fluctuated between 0.28 and 0.30 mV. Addition of 1 μM muscarine, as expected for high depolarization (the situation that prevails when an action potential is applied), did not block release (data not shown). However, 50 μM muscarine produced 63% inhibition within 13 sec.

In PTX-treated preparation, 1 μM muscarine, as before, did not block release (data not shown), whereas 50 μM muscarine produced 35% inhibition within 12 sec (Fig. 6*B*).

On average, 50 μM muscarine reduced the EPSP amplitude within 12 ± 2 sec (n = 8) in untreated and PTX-treated preparations.

Thus, PTX treatment did not block the fast inhibitory effect produced by high concentrations of muscarine.

DISCUSSION

The main findings in this study are: (1) Depolarization affects the functional affinity of the M_2R; the inhibitory effect of muscarine

is less pronounced at higher depolarizing pulses. (2) Feedback inhibition is exerted by two distinct processes. One, PTX-sensitive, is slow and prevails at low to moderate pulse amplitudes, and is of high affinity; low concentrations of muscarine are sufficient to activate it. The second, PTX-insensitive, is fast, voltage-independent, and of low affinity; high concentrations of muscarine are required to activate it. (3) Both these processes, the slow and the fast, are not associated with reduction in Ca^{2+} currents.

How can our results be reconciled with the data showing an M_2-mediated reduction in Ca^{2+} current? As detailed in the introductory remarks, Ca^{2+} currents were measured in cell bodies or in cell lines. Furthermore, long (>100 msec) depolarizing pulses and high agonist concentrations were used. In our studies, Ca^{2+} currents and ACh release were measured concomitantly from the same small release region after brief (0.7 msec) depolarizing pulses or an action potential. Correlating release and Ca^{2+} currents, we found that inhibition of ACh release, even at the highest depolarization, was saturated at 70 μM muscarine, a concentration that did not affect Ca^{2+} influx.

It is possible that the inhibition, reported here, is produced by a direct modulation of the exocytotic machinery. The rapid process may operate via direct coupling between M_2R and proteins of exocytotic machinery (Linial et al., 1997; Ilouz et al., 1999). The slow process, on the other hand, may involve second messenger-mediated modulation of the exocytotic machinery. Such Ca^{2+}-independent presynaptic mechanisms have been implicated in cAMP-dependent modulation of synaptic strength in *Aplysia* (Dale and Kandel, 1990), in crustacean NMJs (Goy and Kravitz, 1989; Delaney et al., 1991), in hippocampus (Capogna et al., 1995; Trudeau et al., 1996), and in the cerebellum (Chen and Regehr, 1997; Kondo and Marty, 1997).

What can be the physiological role of the two inhibitory processes demonstrated here? The high-affinity slow process may serve less as a mean to modulate release, but rather as a safety mechanism that prevents undesired transmitter release under rest conditions. This inhibitory process is active already at low concentrations of ACh, not much higher than the resting concentration of ACh in the synaptic cleft. Furthermore, relief from this inhibition is obtained only at high depolarizations such as the levels produced by an action potential. It follows that even if the terminal is slightly depolarized after repetitive stimulation because of consequent elevation of potassium concentration in the preterminal space, even a small increase in the level of ACh will suffice to prevent undesired continuous release. A similar high-affinity process, also mediated via the M_2R, but operating at resting concentration of ACh, was shown to play a key role in control of release. Slutsky et al. (1999, 2001) showed that the ACh occupied M_2R maintains the release process under tonic block, and high depolarization relieves from that block.

The second fast and low-affinity process, which persists at high depolarizations, may serve to modulate action potential evoked release. After a train of action potentials, the level of transmitter in the synaptic cleft may rise to high levels and consequently release will be inhibited. It is possible that this type of inhibition takes part in various forms of synaptic depression.

We have described here two Ca-independent processes for inhibition of ACh release. But, it is probably the case that in frog, like in many other systems, multiple mechanisms can work together to modify synaptic transmission. For example, inhibition of ACh release in cultured Helisoma neurons was achieved both by reduction of Ca^{2+} current and by direct inhibition of the secretory apparatus (Man-Son-Hing et al., 1989). Also, in Purkinje cells $GABA_B$-mediated inhibition involves decrease in Ca^{2+} entry and, in addition, from Ca^{2+}-independent mechanisms (Dittman and Regehr, 1996). Similarly, in hippocampus and in vertebrate NMJ, adenosine and its agonists inhibited release by reducing Ca^{2+} currents (Miller, 1990; Scholz and Miller, 1991), but also by an additional mechanism (Scholz and Miller, 1992, Silinsky and Solsona, 1992; Redman and Silinsky, 1995).

REFERENCES

Allen TG, Brown DA (1993) M_2 muscarinic receptor-mediated inhibition of the Ca^{2+} current in rat magnocellular cholinergic basal forebrain neurones. J Physiol (Lond) 466:173–189.

Beech DJ, Bernheim L, Hille B (1992) Pertussis toxin and voltage dependence distinguish multiple pathways modulating calcium channels of rat sympathetic neurons. Neuron 8:97–106.

Bellingham MC, Berger AJ (1996) Presynaptic depression of excitatory synaptic inputs to rat hypoglossal motoneurons by muscarinic M_2 receptors. J Neurophysiol 76:3758–3770.

Bernheim L, Beech DJ, Hille B (1991) A diffusible second messenger mediates one of the pathways coupling receptors to calcium channels in rat sympathetic neurons. Neuron 6:859–867.

Birdsall NJM, Burgen ASV, Hulme EC (1978) The binding of agonists to brain muscarinic receptors. Mol Pharmacol 14:723–736.

Brigant JL, Mallart A (1982) Presynaptic currents in mouse motor endings. J Physiol (Lond) 333:619–636.

Capogna M, Gahwiler BH, Thompson SM (1995) Presynaptic enhancement of inhibitory synaptic transmission by protein kinases A and C in the rat hippocampus in vitro. J Neurosci 15:1249–1260.

Caulfield MP (1993) Muscarinic receptors - characterization, coupling and function. Pharmacol Ther 58:319–379.

Chen C, Regehr WG (1997) The mechanism of cAMP-mediated enhancement at a cerebellar synapse. J Neurosci 17:8687–8694.

Dale N, Kandel ER (1990) Facilitatory and inhibitory transmitters modulate spontaneous transmitter release at cultured *Aplysia* sensorimotor synapses. J Physiol (Lond) 421:203–222.

Delaney K, Tank DW, Zucker RS (1991) Presynaptic calcium and serotonin-mediated enhancement of transmitter release at crayfish neuromuscular junction. J Neurosci 11:2631–2643.

Dittman JS, Regehr WG (1996) Contributions of calcium-dependent and calcium-independent mechanisms to presynaptic inhibition at a cerebellar synapse. J Neurosci 16:1623–1633.

Dolezal V, Tućek S (1993) Presynaptic muscarine receptors and the release of acetylcholine from cortical prisms: roles of Ca^{2+} and K^+ concentration. Naunyn Schmiedebergs Arch Pharmacol 348:228–233.

Dudel J (1981) The effect of reduced calcium on quantal unit current and release at the crayfish neuromuscular junction. Pflügers Arch 391:35–40.

Dudel J, Parnas I, Parnas H (1993) Spatial facilitation and depression within one motor nerve terminal of frogs. J Physiol (Lond) 461:119–131.

Goy MF, Kravitz EA (1989) Cyclic AMP only partially mediates the actions of serotonin at lobster neuromuscular junctions. J Neurosci 9:369–379.

Hamilton BR, Smith DO (1991) Autoreceptor-modulated purinergic and cholinergic inhibition of motor nerve terminal calcium currents in the rat. J Physiol (Lond) 432:327–341.

Herlitze S, Garcia DE, Mackie K, Hille B, Scheuer T, Catterall WA (1996) Modulation of Ca^{2+} channels by G-protein $\beta\gamma$ subunits. Nature 380:258–262.

Hille B (1994) Modulation of ion-channel function by G-protein-coupled receptors. Trends Neurosci 17:531–535.

Ikeda SR (1996) Voltage-dependent modulation of N-type calcium channels by G-protein beta gamma subunits. Nature 380:255–258.

Ilouz N, Branski L, Pranis J, Parnas H, Linial M (1999) Depolarization affects the binding properties of muscarinic acetylcholine receptors and their interaction with proteins of the exocytic apparatus. J Biol Chem 274:29519–29528.

Kondo S, Marty A (1997) Protein kinase A-mediated enhancement of miniature IPSC frequency by noradrenaline in rat cerebellar stellate cells. J Physiol (Lond) 498:165–176.

Linial M, Ilouz N, Parnas H (1997) Voltage-dependent interaction between the muscarinic ACh receptor and proteins of the exocytic machinery. J Physiol (Lond) 504:251–258.

Man-Son-Hing H, Zoran MJ, Lukowiak K, Haydon PG (1989) A neuromodulator of synaptic transmission acts on the secretory apparatus as well as on ion channels. Nature 341:237–239.

McKinney M, Anderson D, Vella-Rountree L (1989) Different agonist-receptor active conformations for rat brain M_1 and M_2 muscarinic receptors that are separately coupled to two biochemical effector systems. Mol Pharmacol 35:39–47.

Miller RJ (1990) Receptor-mediated regulation of calcium channels and neurotransmitter release. FASEB J 4:3291–3299.
Muller D, Loctin F, Dunant Y (1987) Inhibition of evoked acetylcholine release: two different mechanisms in the Torpedo electric organ. Eur J Pharmacol 33:225–234.
Patil PG, de Leon M, Reed RR, Dubel S, Snutch TP, Yue DT (1996) Elementary events underlying voltage-dependent G-protein inhibition of N-type calcium channels. Biophys J 71:2509–2521.
Ravin R, Spira ME, Parnas H, Parnas I (1997) Simultaneous measurement of intracellular Ca^{2+} and asynchronous transmitter release from the same crayfish bouton. J Physiol (Lond) 501:251–262.
Redman RS, Silinsky EM (1995) On the simultaneous electrophysiological measurements of neurotransmitter release and perineural calcium currents from frog motor nerve endings. J Neurosci Methods 57:151–159.
Roche JP, Treistman SN (1998) Ca^{2+} channel $\beta 3$ subunit enhances voltage-dependent relief of G-protein inhibition induced by muscarinic receptor activation and $G_{\beta\gamma}$. J Neurosci 18:4883–4890.
Rouse ST, Levey AI (1997) Muscarinic acetylcholine receptor immunoreactivity after hippocampal commissural/associational pathway lesions: evidence for multiple presynaptic receptor subtypes. J Comp Neurol 380: 382–394.
Rouse ST, Edmunds SM, Yi H, Gilmor ML, Levey AI (2000) Localization of M(2) muscarinic acetylcholine receptor protein in cholinergic and non-cholinergic terminals in rat hippocampus. Neurosci Lett 284:182–186.
Scanziani M, Gahwiler BH, Thompson SM (1995) Presynaptic inhibition of excitatory synaptic transmission by muscarinic and metabotropic glutamate receptor activation in the hippocampus: are Ca^{2+} channels involved? Neuropharmacology 34:1549–1557.
Scholz KP, Miller RJ (1991) Analysis of adenosine actions on Ca^{2+} currents and synaptic transmission in cultured rat hippocampal pyramidal neurones. J Physiol (Lond) 435:373–393.
Scholz KP, Miller RJ (1992) Inhibition of quantal transmitter release in the absence of calcium influx by a G protein-linked adenosine receptor at hippocampal synapses. Neuron 8:1139–1150.
Silinsky EM, Solsona CS (1992) Calcium currents at motor nerve endings: absence of effects of adenosine receptor agonists in the frog. J Physiol (Lond) 457:314–328.
Slutsky I, Parnas H, Parnas I (1999) Presynaptic effects of muscarine on ACh release at the frog neuromuscular junction. J Physiol (Lond) 514:769–782.
Slutsky I, Silman I, Parnas H, Parnas I (2001) Presynaptic M_2 muscarinic receptors are involved in controlling the kinetics of ACh release at the frog neuromuscular junction. J Physiol (Lond) 536:717–725.
Starke K, Göthert M, Kilbinger H (1989) Modulation of neurotransmitter release by presynaptic autoreceptors. Physiol Rev 69:864–989.
Trudeau LE, Doyle RT, Emery DG, Haydon PG (1996) Calcium-independent activation of the secretory apparatus by ruthenium red in hippocampal neurons: a new tool to assess modulation of presynaptic function. J Neurosci 16:46–54.
Zamponi GW, Snutch TP (1998) Modulation of voltage-dependent calcium channels by G proteins. Curr Opin Neurobiol 8:351–356.
Zamponi GW, Bourinet E, Nelson D, Nargeot J, Snutch TP (1997) Crosstalk between G proteins and protein kinase C mediated by the calcium channel $\alpha 1$ subunit. Nature 385:442–446.
Zhang JF, Ellinor PT, Aldrich RW, Tsien RW (1996) Multiple structural elements in voltage-dependent Ca^{2+} channels support their inhibition by G proteins. Neuron 17:991–1003.